Electronic Supplementary Material (ESI) for Chemical Science.

Supporting Information

Visible-light Harvesting Pyrene-based MOFs as Efficient ROS Generators

Yingmu Zhang[a], Jiandong Pang[a], Jialuo Li[a], Xinyu Yang[a], Mingbao Feng[c], Peiyu Cai[a], Hong-Cai Zhou*[,a,b]

[a] Department of Chemistry, Texas A&M University, College Station, Texas 77842-3012, United States.

[b] Department of Materials Science and Engineering, Texas A&M University, College Station, Texas 77842, United States.

[c] Department of Environmental and Occupational Health, School of Public Health, Texas A&M University, College Station, TX 77843, United State.

*Correspondence Author:
Dr. Hong-Cai Zhou
Email: zhou@chem.tamu.edu

Table of Contents

S1. Materials and Instrumentation

Materials

All commercially available reagents and solvents were purchased from either VWR or Sigma Aldrich. Unless otherwise noted, they were used without further purification.

Instrumentation

Powder X-ray diffraction (PXRD) was carried out on a Bruker D8-Focus Bragg-Brentano X-ray powder diffractometer equipped with a Cu microfocus tube (λ = 1.54178 Å) at 40 kV and 40 mA. Single crystal X-ray diffraction experiments were carried out on a Brucker D8-Venture or D8 Quest diffractometer equipped with a Mo-Kα sealed-tube X-ray source (λ = 0.71073 Å, graphite monochromated) at low temperature device (100 K). IR spectrum was performed in the range 4000-400 cm^{-1} using KBr pellets on a Gas Chromatography Fourier Transform Infrared Spectrometer (NEXUS670). Thermogravimetric analysis (TGA) were carried out on a Shimadzu TGA-50 thermogravimetric analyzer from temperature to 600 °C at a ramp rate of 5 °C/min in a flowing air atmosphere. Nuclear magnetic resonance (NMR) data were collected on a Mercury 500 spectrometer. The electronic absorption spectra were recorded on a Hitachi U-4100 UV-Vis-NIR spectrophotometer. Solid-state fluorescence spectra were recorded on a F-7000 FL spectrophotometer equipped with a xenon lamp and quartz carrier at room temperature. Electron Paramagnetic Resonance (EPR) measurement was conducted on a Bruker Elexsys II E500 EPR spectrometer equipped with a Bruker ER4131VT variable-temperature unit. Confocal scanning microscopic images were obtained by Leica TCS SP8 confocal microscope equipped with a motorized xy stage and epifluorescence illumination.

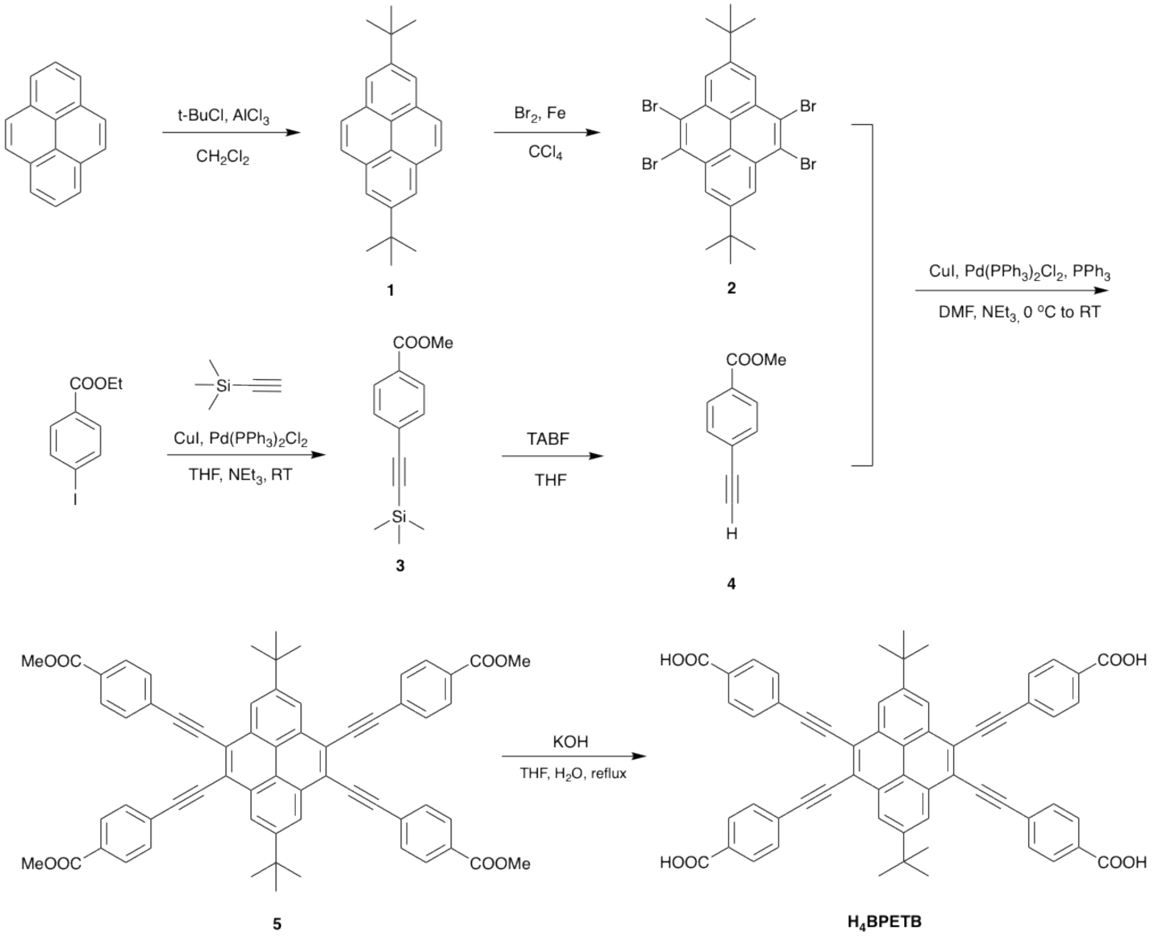

Scheme S1. Synthesis procedure of H_4BPETB.

S2. Synthesis of Ligand H_4BPETB

Synthesis of 2,7-di-tert-butylpyrene (1)

In a 500 mL three-necked round-bottom flask, pyrene (10.1 g, 50 mmol) and $AlCl_3$ (0.6 g, 4.5 mmol) were added into 200 mL anhydrous CH_2Cl_2. Then tert-butyl chloride (10.2 g diluted in 75 mL CH_2Cl_2) was added into the solution drop by drop at 0 °C under N_2. The mixture was then allowed to react at room temperature for 6 h. After that, iced water with 25 mL HCl was poured into the mixture and the organic phase was washed with water three times and separated. The solvent was pumped out and the resulted solids were further purified by chromatography with hexane as eluent to give pure white solid (14.6 g, 46.4 mmol, 93%). ^{1}H NMR (500 MHz, $CDCl_3$) δ 8.19 (s, 4H), 8.03 (s, 4H), 1.59 (s, 18H).

Synthesis of 2,7-di-tert-bultyl-4,5,9,10-tetrabromopyrene (2)

In a 500 mL round-bottom flask, **1** (4.0 g, 12.7 mmol) and iron powder (4.0 g) was added in 150 mL CCl_4. Liquid bromine (12.4 g, 78 mmol) in 40 mL CCl_4 was then added dropwise into the mixture. The reaction mixture was then allowed to react for 4 h at room temperature. After that, 100 mL saturated aqueous $Na_2S_2O_3$ solution was poured into the system and the mixture was stirred for another couples of hours until the color turned to pale pink. The organic layer was then separated and washed with water three times. The solvent was removed under vacuum and the obtained solid was further recrystallized in benzene to afford white product (5.6 g, 8.9 mmol, 70%). ^{1}H NMR (500 MHz, $CDCl_3$) δ 8.87 (s, 4H), 1.63 (s, 18H).

Synthesis of methyl 4-((trimethylsilyl)ethynyl)benzoate (3)

Ethyl-4-iodobenzoate (13.5 g, 50 mmol), $Pd(PPh_3)_2Cl_2$ (1.5 g, 2.1 mmol) and CuI (290 mg, 1.5 mmol) were added in a 500 mL three-necked round bottle flask. The flask was fitted on a schlenk line followed by vacuumed and refilled with N_2 three times. A mixture of Et_3N/THF (v/v = 150 mL/150 mL) was bubbled with N_2 for 30 min and then transferred to the flask through a canula. Trimethylsilyl acetylene (8.5 mL, 60 mmol) was then added into the system by syringe. The reaction mixture was then stirred at room temperature under the protection of N_2 for 5 h. After that, the solvent was removed under vacuum and the crude product was purified by a short column (eluent: EtOAc/hexane = 1/6) to give dark yellow solid (10.5 g, 42.5 mmol, 85 %). ^{1}H NMR (500 MHz, $CDCl_3$) δ 7.95 (d, *J* = 8.1 Hz, 2H), 7.49 (d, *J* = 8.0 Hz, 2H), 3.93 (s, 3H), 0.24 (s, 9H).

Synthesis of methyl 4-ethynylbenzoate (4)

In a 500 mL round-bottom flask, **3** (10.0 g, 40 mmol) was dissolved in 200 mL THF followed by addition of 40 mL tetrabutylammonium fluoride solution (TBAF, 1.0 M in THF). The reaction mixture was then stirred at room temperature for 15 min. The solvent was removed and the crude product was purified by a short column (eluent: EtOAc/hexane = 1/5) to give light yellow solid (6.26 g, 36 mmol, 90%). ^{1}H NMR (500 MHz, $CDCl_3$) δ 8.00 (d, *J* = 8.7 Hz, 2H), 7.56 (d, *J* = 8.5 Hz, 2H), 3.93 (s, 3H), 3.23 (s, 1H).

Synthesis of tetramethyl 4,4',4'',4'''-((2,7-di-tert-butylpyrene-4,5,9,10-tetrayl)tetrakis(ethyne-2,1-diyl))tetrabenzoate (Me_4BPETB).

2 (400 mg, 0.64 mmol), $Pd(PPh_3)_2Cl_2$ (90 mg, 0.13 mmol), CuI (24.4 mg, 0.13 mmol) and PPh_3 (67.2 mg, 0.26 mmol) were added in a 250 mL three-necked round bottle flask fitted on a Schlenk line. The flask was vacuumed and refilled with N_2 three times and a mixture of DMF/THF (v/v = 60 mL/60 mL) was transferred to the flask through a canula after bubbled with N_2 for 30 min. The reaction mixture was stirred for 30 min at 0 °C under N_2 and **4** (891 mg, 5.12 mmol) was added by a syringe. The mixture was then heated up to 100 °C and allowed to react for another 48 h. After cooling to room temperature, the mixture was poured into a large amount of water and extracted with $CHCl_3$ three times. The organic phase was collected and washed with saturated aqueous NH_4Cl, H_2O and brine successively. The organic layer was then dried with $MgSO_4$ and the organic solvent was removed under vacuum. The crude product was then purified by a short column (eluents: from hexane/chloroform = 2/1 to pure chloroform). The obtained solid was further washed with methanol to afford yellow solid (400 mg, 0.456 mmol, 71 %). ^{1}H NMR (500 MHz, $CDCl_3$) δ 8.91 (s, 4H), 8.15 (d, J = 7.3 Hz, 8H), 7.83 (d, J = 7.1 Hz, 8H), 3.99 (s, 12H), 1.70 (s, 18H).

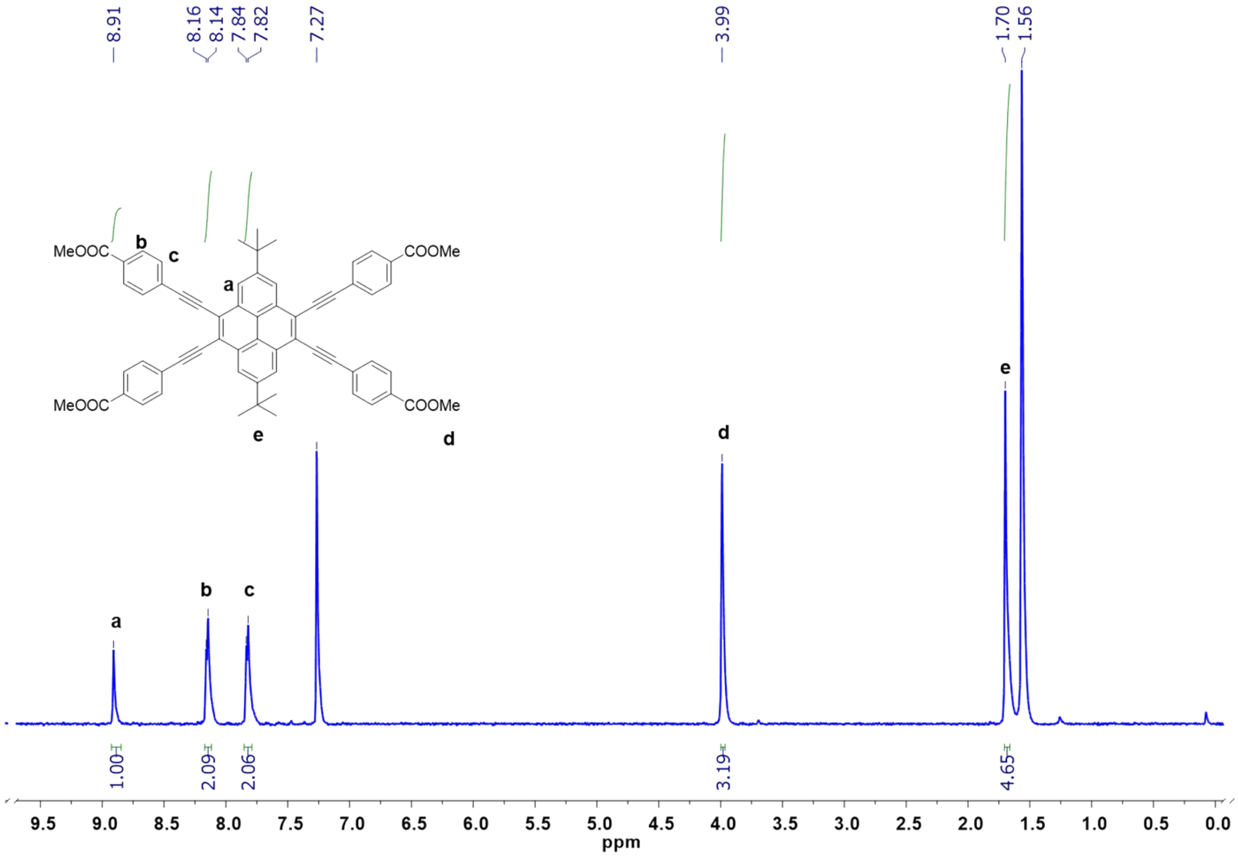

Fig. S1. ^{1}H NMR spectrum of H$_4$BPETB.

Synthesis of 4,4',4'',4'''-((2,7-di-tert-butylpyrene-4,5,9,10-tetrayl)tetrakis(ethyne-2,1-diyl))-tetrabenzoic acid (H$_4$BPETB)

5 (400 g, 0.46 mmol) and potassium hydroxide (2.4 g, 43.7 mmol) were added into a mixture of THF/water (v/v = 50 mL/50mL) and was refluxed overnight. After cooling, the organic solvent was removed and the aqueous phase was acidified with 6 M hydrochloric acid to give yellow precipitate, which was then washed with water several times and dried under vacuum (354 mg, 0.4 mmol, 90%). Due to its low solubility in common deuterium-solvents, the product was used directly to synthesize MOF without further characterization.

S3. Synthesis of PCN-822

PCN-822(Zr)

In a 4 mL Pyrex vial, $ZrCl_4$ (10 mg, 0.043 mmol), H_4BPETB (5mg, 0.006 mmol) and 290 µL trifluoroacetic acid (TFA) were ultrasonically dissolved in 2 mL N, N-dimethylformamide (DMF). The mixture was then heated in a 120 °C oven for 4 days to afford yellow crystals (Yield: 3mg). The crystals were further washed with DMF three times and were allowed to stay in fresh DMF for further structural characterization.

PCN-822(Hf)

In a 4 mL Pyrex vial, $HfCl_4$ (10 mg, 0.032), H_4BPETB (5 mg, 0.006 mmol) and 280 µL trifluoroacetic acid (TFA) were ultrasonically dissolved in 2 mL N, N-dimethylformamide (DMF). The mixture was then heated in a 120 °C oven for 4 days to afford yellow crystals (Yield: 3 mg). The crystals were further washed with DMF three times and were allowed to stay in fresh DMF for further structural characterization.

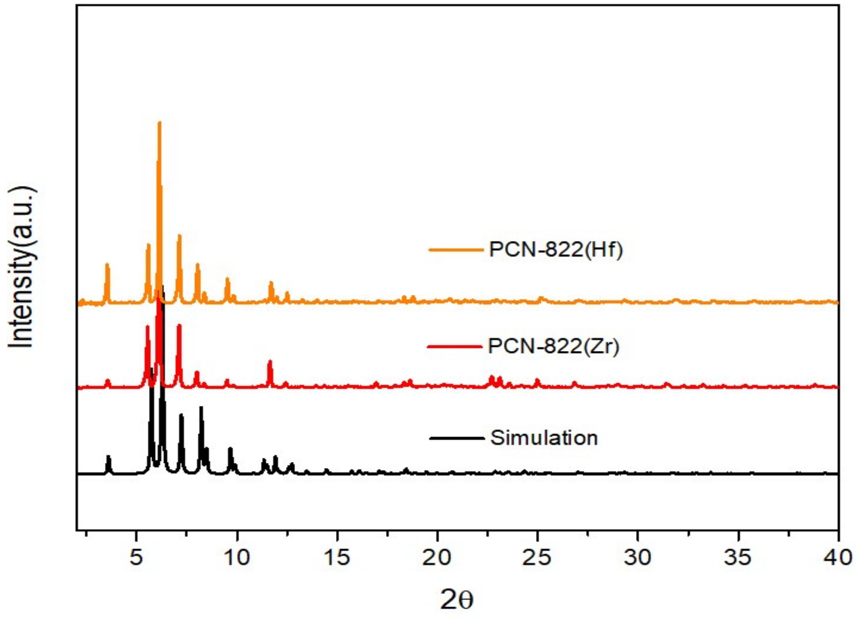

Fig. S2. Powder X-ray diffraction (PXRD) patterns of as-synthesized PCN-822 (Zr) in red, PCN-822(Hf) in orange and the simulated pattern in black.

S4. Single Crystal X-ray Crystallography

The single-crystal was taken from the mother liquid without further treatment, transferred to oil and mounted into a loop for single crystal X-ray data collection. Diffraction was measured on a Bruker D8 Venture or D8 Quest diffractometer equipped with a Cu-Kα sealed-tube X-ray source (λ = 1.54184 Å, graphite monochromated) at low temperature device (100 K). The data frames were recorded using the program APEX3 and processed using the program *SAINT* routine within APEX3. The data were corrected for absorption and beam corrections based on the multi-scan technique as implemented in *SADABS*. The structures were solved by direct methods using *SHELXS* and refined by full-matrix least-squares on F^2 using *SHELXL* software. [1] Crystal data are summarized in Table S1. CCDC 1908132 contain the supplementary crystallographic data for this paper. These data can be obtained free of charge from The Cambridge Crystallographic Data Centre.

Table S1. Crystal data and structure refinements for PCN-822 (Zr)

code	**PCN-822(Zr)**
CCDC	1908132
formula	$C_{57}H_{28}O_{16}Zr_3$
Mw	1242.45
T / K	100(2)
Crystal system	tetragonal
Space group	$I4_1/amd$
a / Å	15.0920(12)
c / Å	98.494(7)
V / Å^3	22434(4)
Z	8
D_c / g cm^{-3}	0.736
μ (mm^{-1})	2.529
F (000)	4944
Completeness	0.988
Collected reflections	4617
Unique reflections	2083
Parameters	57
R_{int}	0.1176
R_1[I＞2σ]	0.1121
wR_2[I＞2σ]	0.3190
R_1 (all data)	0.1655
wR_2 (all data)	0.3561
GOF on F^{20}	1.056

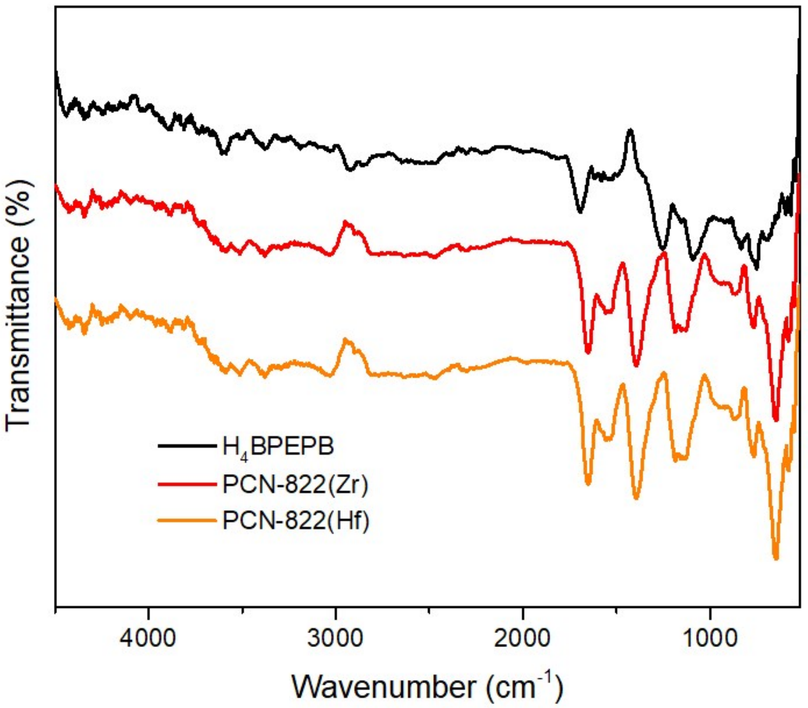

Fig. S3. FT-IR spectra of ligand (black) and PCN-822(Zr/Hf).

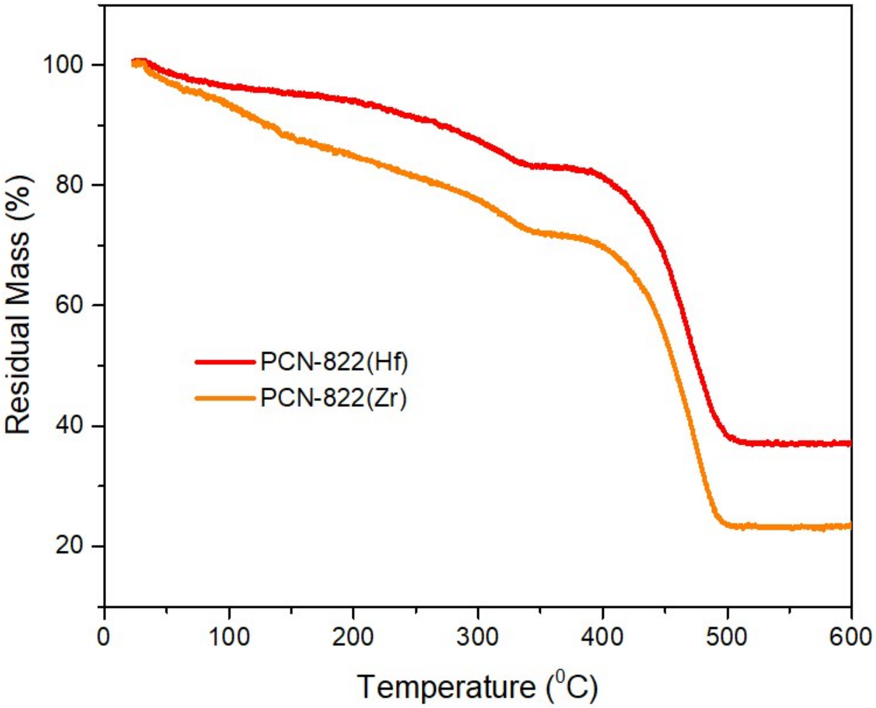

Fig. S4. Thermogravimetric (TG) analysis data of as-synthesized PCN-822(Zr/Hf).

S5. Thermogravimetric Analysis and Chemical Stability Tests

~ 50 mg MOFs were immersed into the aqueous solutions with pH values from 1-11 respectively prepared by NaOH as base and HCl as acid and the samples were allowed to stay overnight.

Afterwards, the samples were filtered, dried and weighed before the powder X-ray diffraction tests. The MOFs show trivial loss of weigh and the PXRD patterns remain unchanged.

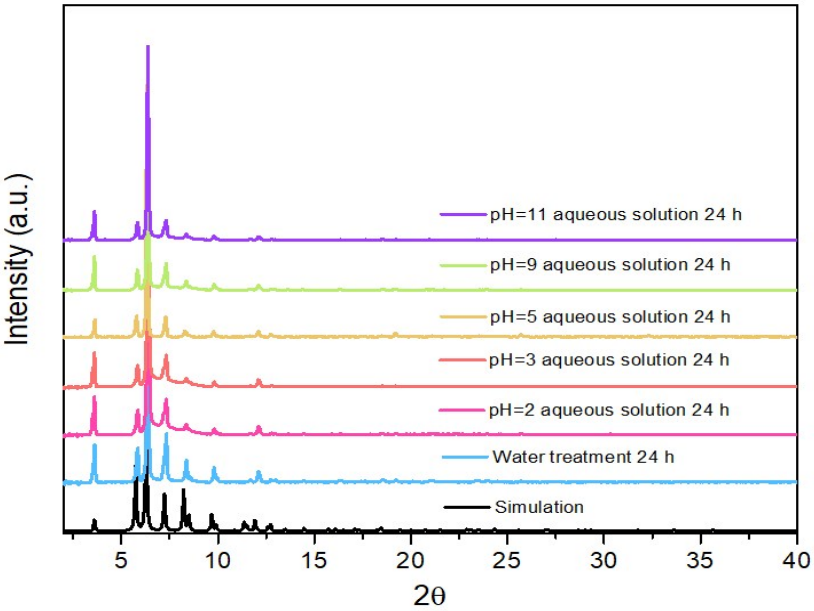

Fig. S5. PXRD patterns of PCN-822(Zr) in aqueous solutions with various pH values.

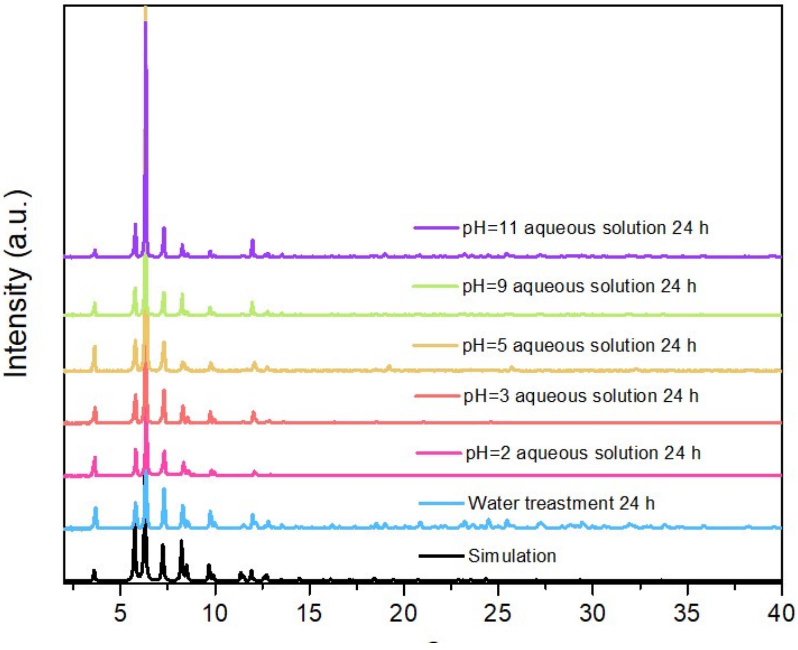

Fig. S6. PXRD patterns of PCN-822(Hf) in aqueous solutions with various pH values.

S6. Porosity

Both regular activation process by the 'outgas' function of Micrometritics ASAP 2020 system the supercritical CO_2 condition under various temperature and times as well as the supercritical CO_2 condition have been tried to activate the MOFs for N_2 isotherm uptake measurements. As the activation attempts were unsuccessful, instead, the porosity of the materials was confirmed by dye adsorption in solution.

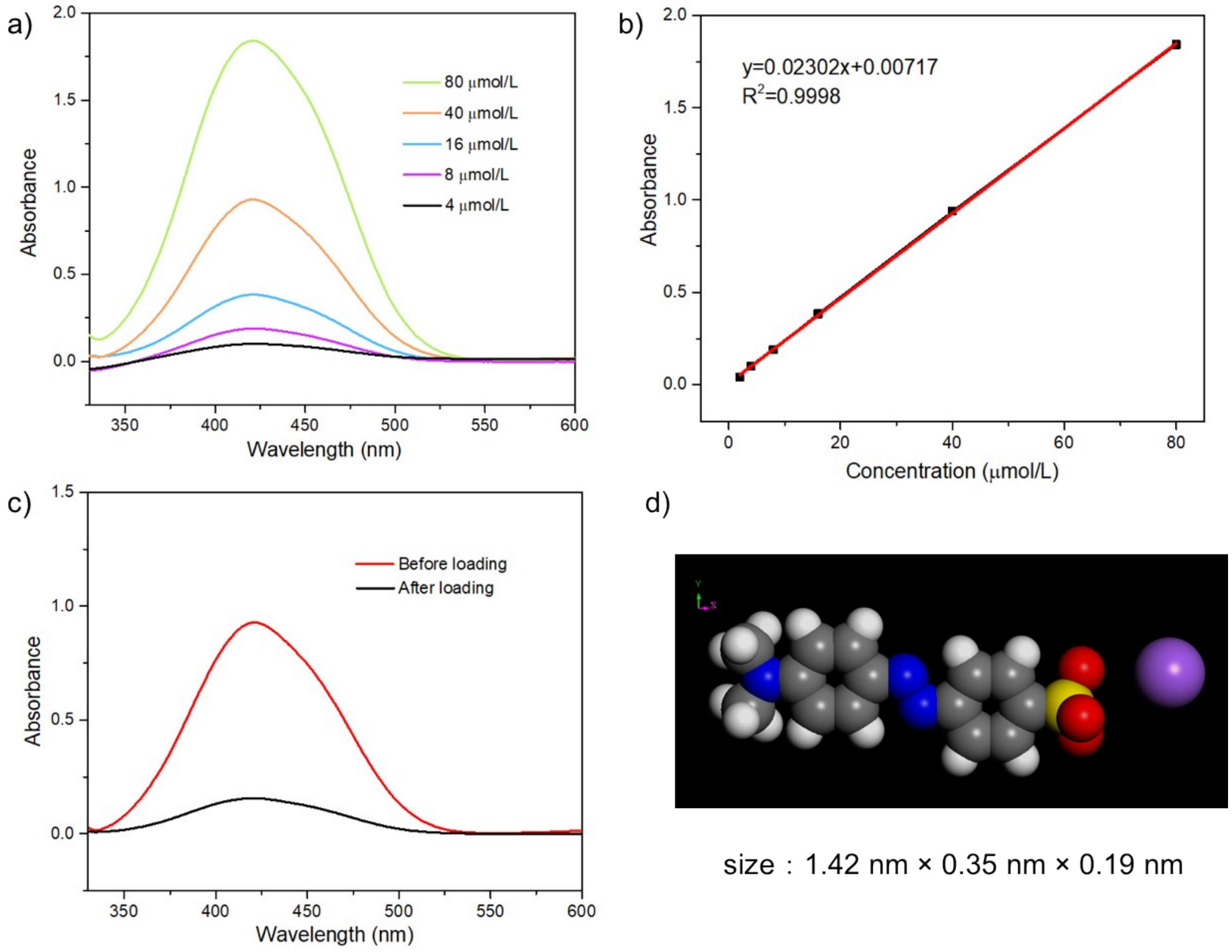

Fig. S7. a) UV-vis. spectra of methyl orange solutions with various concentrations. b) Calibration curve obtained based on the UV-vis spectra. c) The change of UV-vis spectra of methyl orange solution before and after loading PCN-822(Zr/Hf). d) 3D structure of methyl orange.

n(MO) = V × (C_{before} − C_{after}) = (4000 − 646) × 10^{-6} M × 3.00 × 10 $^{-3}$ L = 10. 1 × 10^{-6} mol;

n(MOF) = 12.8 mg/M.W = 4.78 × 10^{-6} mol;

n(MO) : n (MOF) ≈ 2

S7. Photophysical Properties

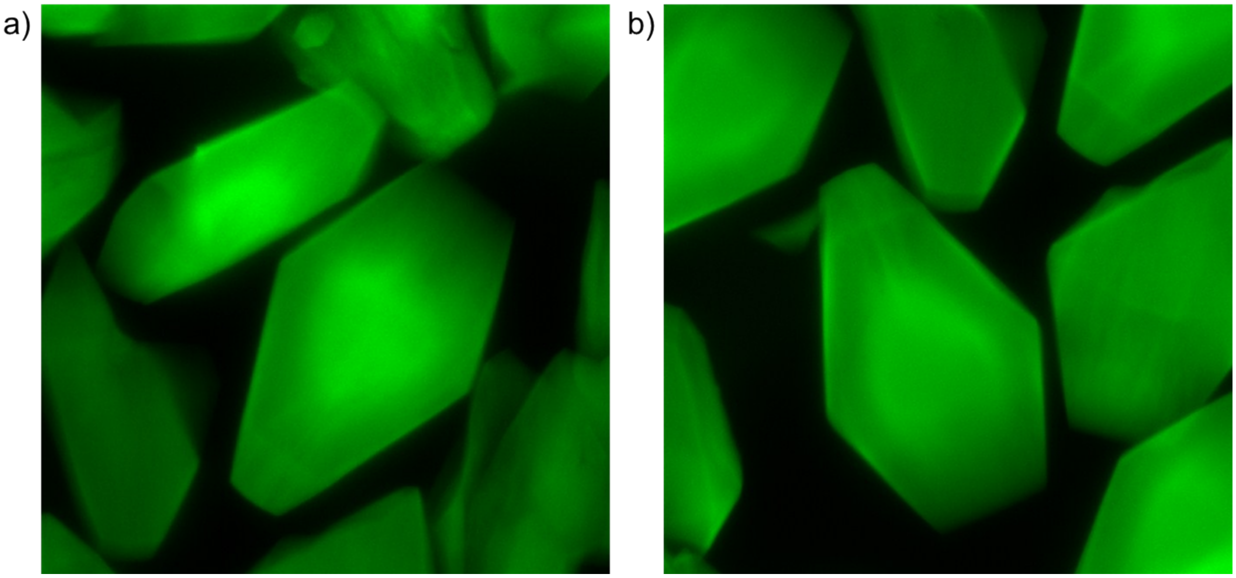

Fig. S8. Confocal scanning microscopic images of a) PCN-822(Zr) and b) PCN-822(Hf).

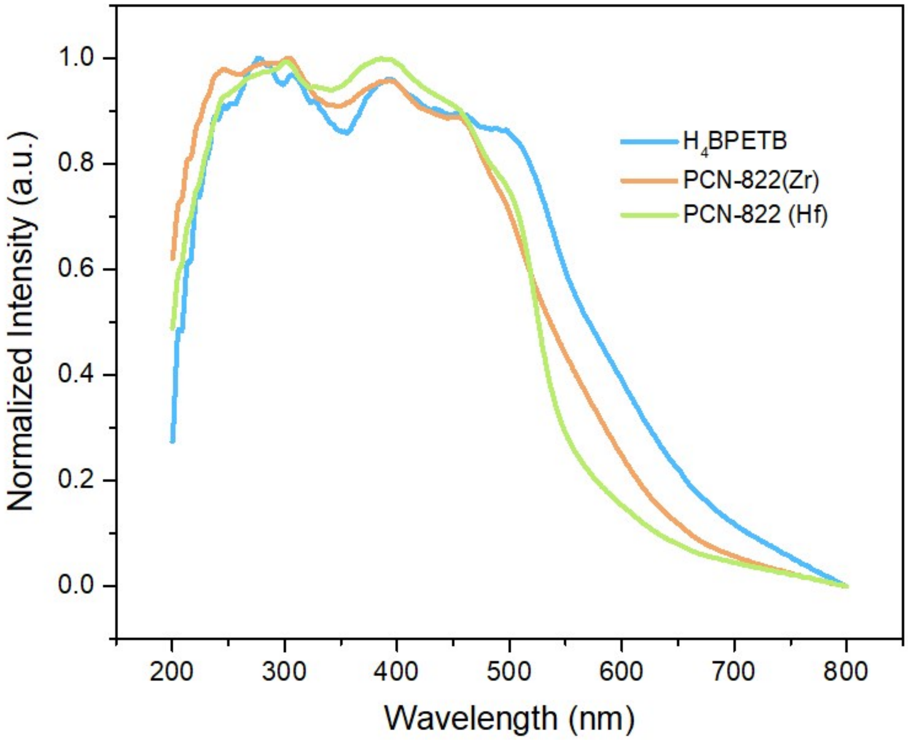

Fig. S9. Solid-state UV-vis absorption spectra of ligand and PCN-822(Zr/Hf).

The optical band gaps were also computed using Tauc plot based on the solid-state absorption spectra.

$$(h\nu\alpha)^2 = A\ (h\nu - Eg)$$

h: Planck's constant, *v*: frequency of vibration, α: absorption coefficient, Eg: band gap, A: proportional constant.

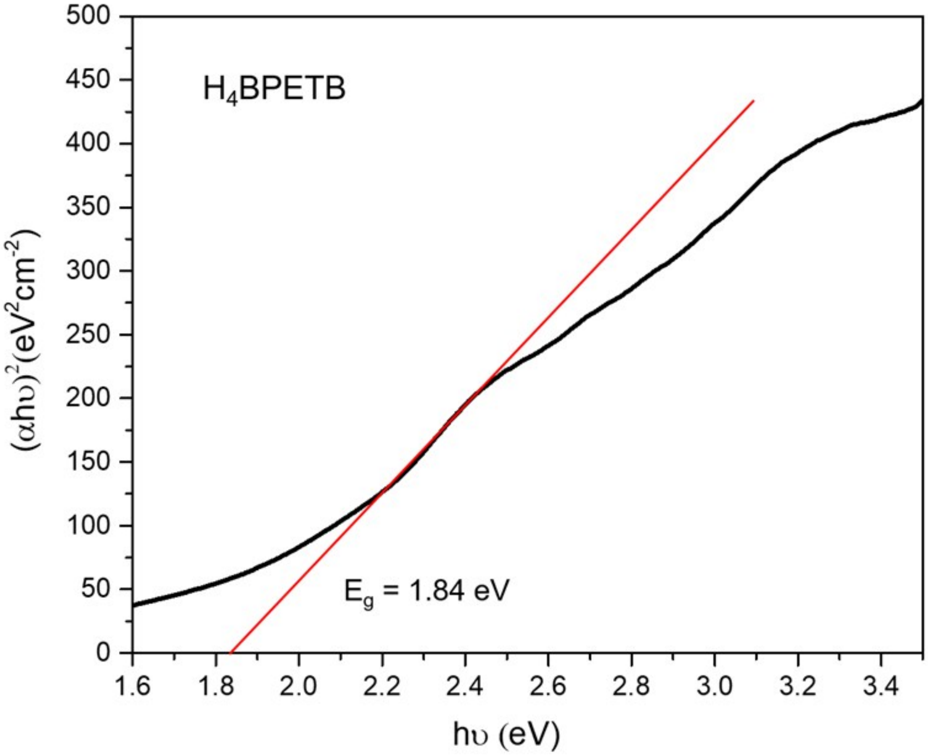

Fig. S10. Tauc plot of H_4BPETB. The optical band gap of is calculated to be 1.84 eV.

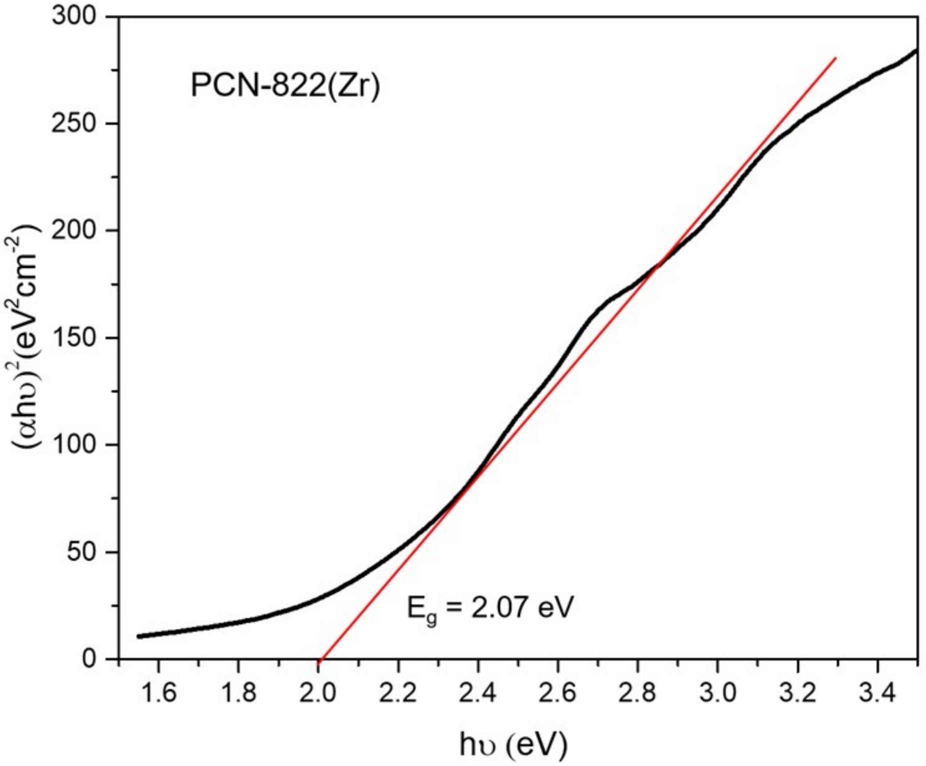

Fig. S11. Tauc plot of PCN-822(Zr). The optical band gap of is calculated to be 2.07 eV.

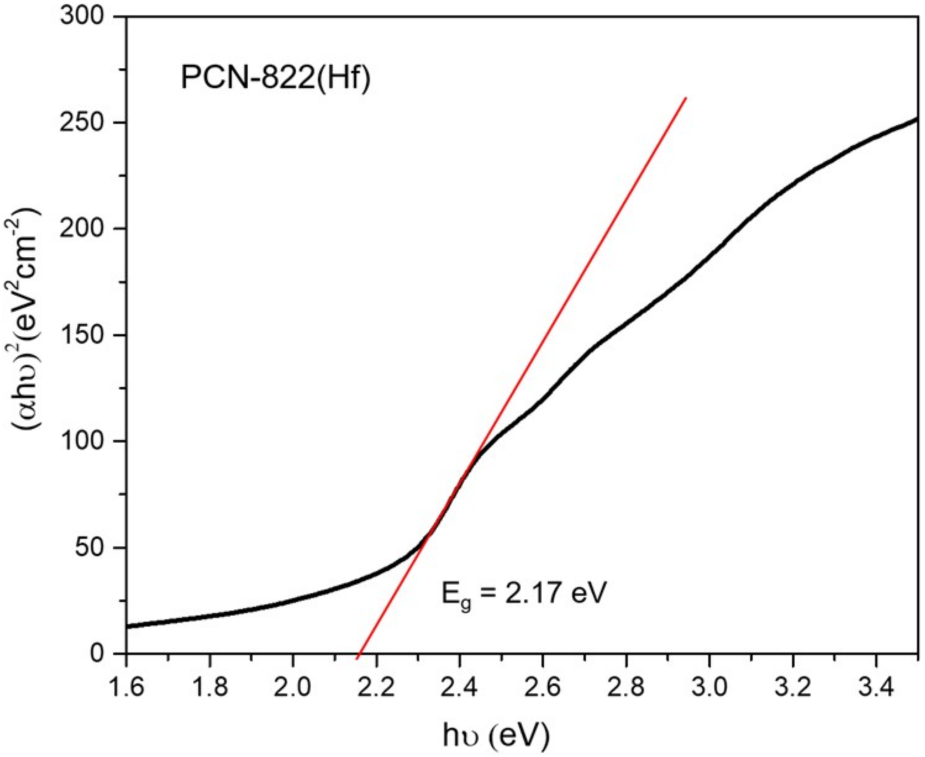

Fig. S12. Tauc plot of PCN-822(Hf). The optical band gap of is calculated to be 2.17 eV.

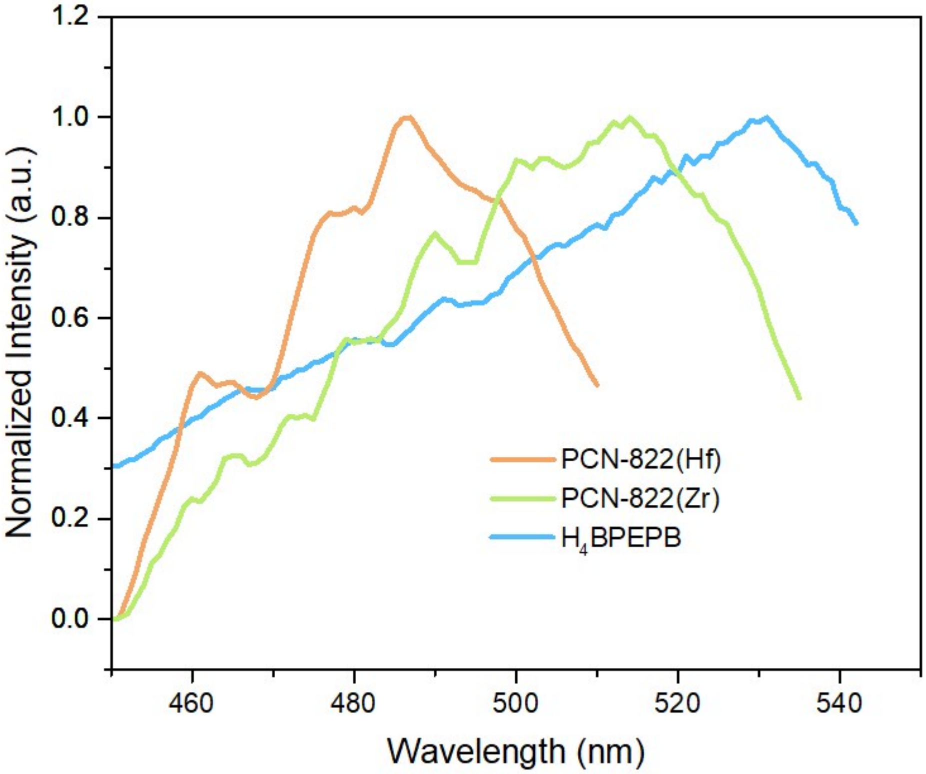

Fig. S13. Excitation spectra of ligand and PCN-822(Zr/Hf).

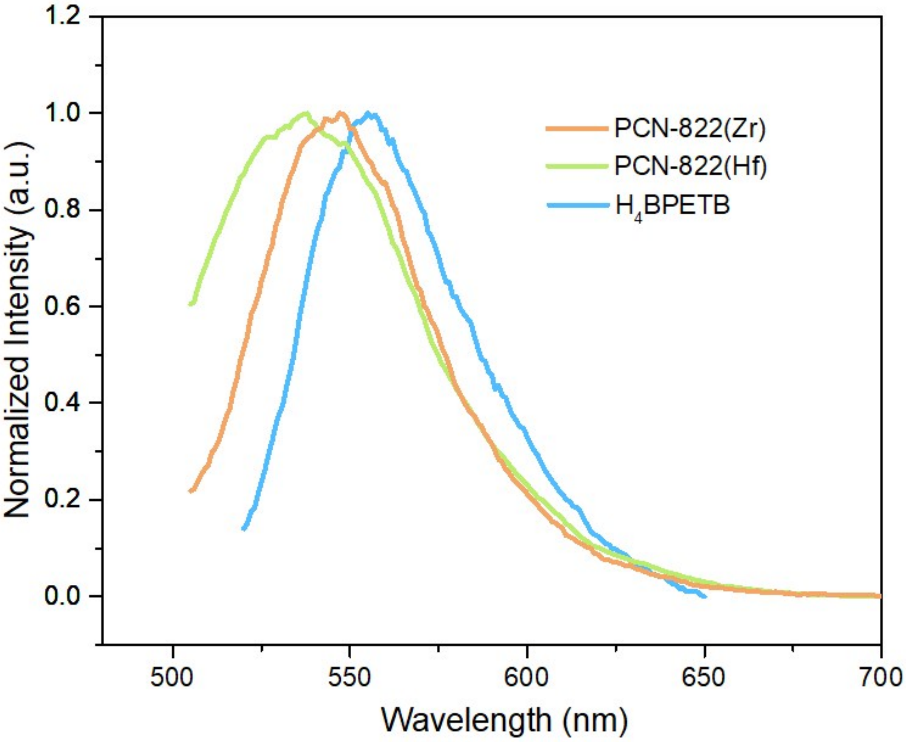

Fig. S14. Emission spectra of ligand and PCN-822(Zr/Hf).

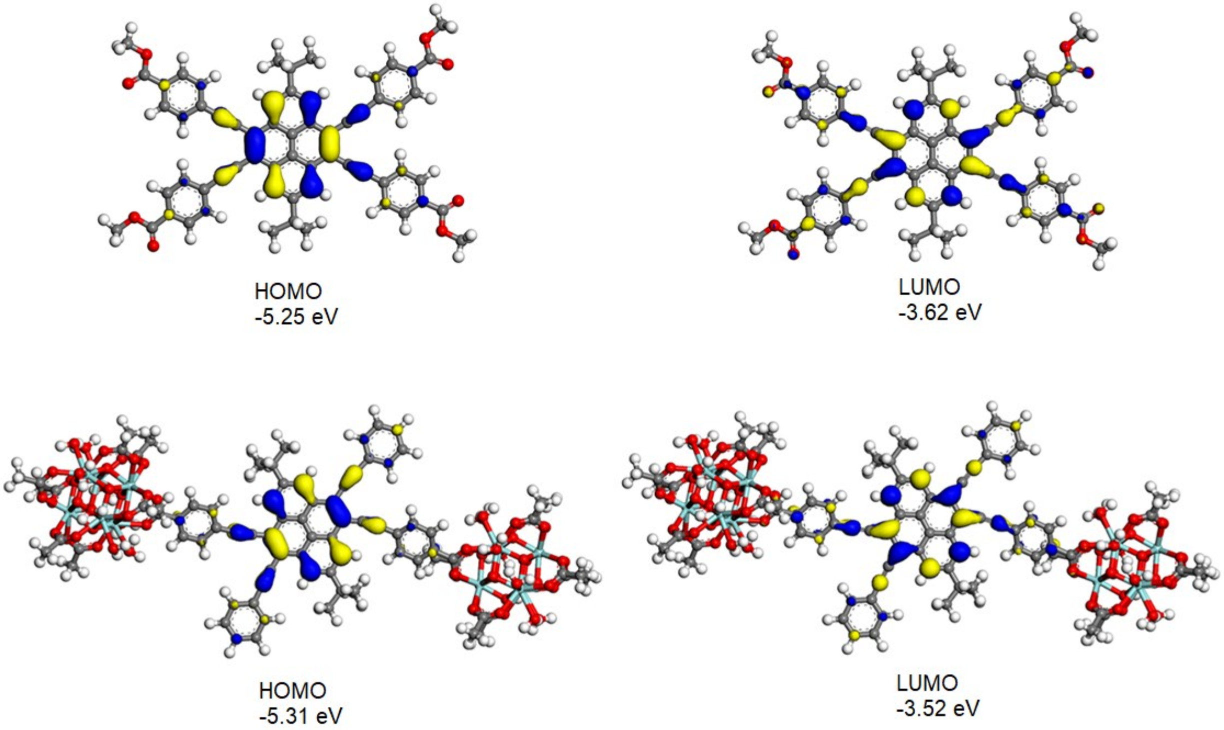

Fig. S15. The frontier molecular orbital distribution of free organic ligand (up) and in PCN-822.

S8. Photooxidation of 1,5-Dihydroxynaphthalene (DHN)

In a 4 mL Pyrex vial, the reactions were carried out with 0.036 mmol of DHN and 1 mmol % PCN-822(Zr/Hf) in 3 mL acetonitrile under the irradiation of visible light and the UV-vis absorption of the mixture was recorded at an interval of one hour.

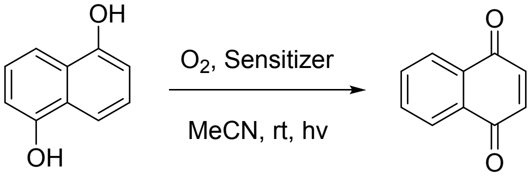

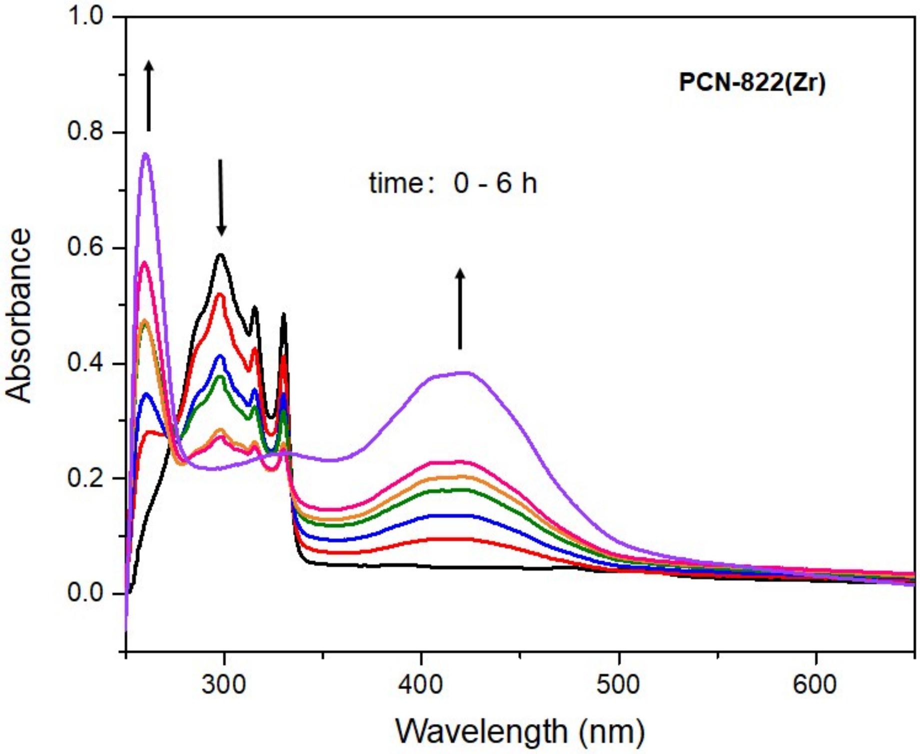

Fig. S16. UV-vis absorption spectral change for photooxidation of DHN with PCN-822(Zr) as sensitizer.

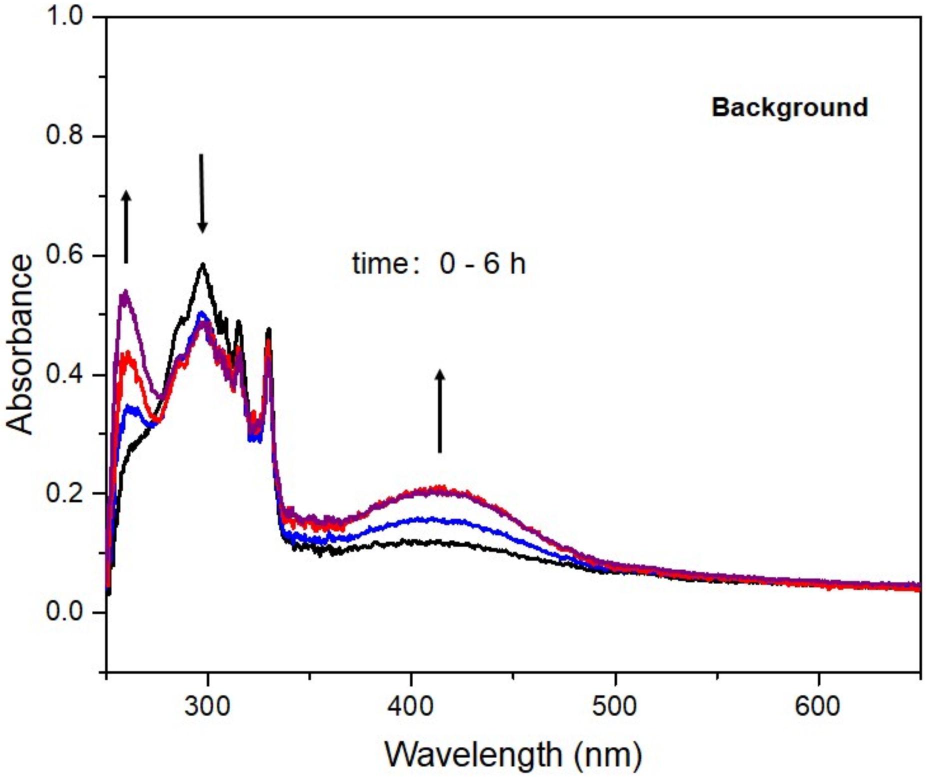

Fig. S17. UV-vis absorption spectral change for photooxidation of DHN with no sensitizer.

S9. General Procedure for the Oxidation of Amines

Before photocatalytic studies, the as-synthesized MOFs washed with the acetone three times and dried. Then the MOF power was added to the corresponding solvents (acetonitrile for example) for further photocatalytic reactions. In a 4 mL Pyrex vial was added amines (0.2 mmol) and powder PCN-822 (~1 mmol %). The vial was capped with a septum stopper and 2.0 mL solution was added with a syringe. The mixture was then bubbled with O_2 for 30 min and stirred under an oxygen atmosphere (1 atm) at room temperature for another 12 h upon the irradiation of LED light (λ = 450 nm), 100 mW/cm^2. Afterwards, the solid was removed by filtration and washed with dichloromethane twice. The filtrate was collected and the organic solvent was then removed under vacuum to afford residual for ^{1}H NMR characterization.

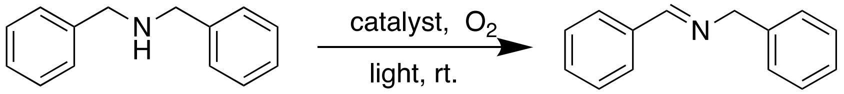

Table S2. Screening experiments of oxidation of dibenzylamine[a]

Entry	Catalyst (mol %)	Solvent	t (h)	Yield (%)
1	PCN-822(Hf) (0.5 %)	dichloromethane	6 h	15
2	PCN-822(Hf) (0.5 %)	ethyl acetate	6 h	30.3
3	PCN-822(Hf) (0.5 %)	acetonitrile	6 h	66
4	PCN-822(Hf) (0.5 %)	chloroform	6 h	< 5
5	PCN-822(Hf) (0.5 %)	THF	6 h	36.9
4	PCN-822(Hf) (0.5 %)	acetonitrile	12 h	51
6	PCN-822(Hf) (1.0 %)	acetonitrile	6 h	79
7[b]	PCN-822(Hf) (1.0 %)	acetonitrile	6 h	—
8[c]	PCN-822(Hf) (1.0 %)	acetonitrile	6 h	—
9	—	acetonitrile	6 h	—
10	$Me_4BPETB/HfCl_4$ (1.0%)	acetonitrile	6 h	22.2

[a] Reaction conditions: dibenzylamine (0.1 mmol), catalyst, solvent (2.0 mL), 1 atm O_2, rt., LED light (λ = 450 nm), 100 mW/cm^2. [b] Without light. [c] Under 1 atm N_2. Yields were determined by ^{1}H NMR with mesitylene as internal standard.

Table S3. Comparison of aerobic dibenzylamine oxidation with selective photocatalysts.

Entry	Photocatalyst	Time (h)	Yields (%)	Light source	Ref.
1	WS_2	36	63	white LED, 60 W	[2]
2	TiO_2	8	91	Hg lamp (λ>300 nm), 100 W	[3]
3	mpg-C_3N_4	2	70	Xe lamp (λ > 420 nm), 300 W	[4]
4	Ru^{II}(TDCPP)(CO)	8	>99	tungsten lamp, 300W	[5]
5	H_2TPrPc	1	>99	LED (λ = 440 nm), 3W	[6]
6	$Ru(bpy)_3$	1	58	Xe Lamp (λ > 380 nm), 20 mW/cm^2	[7]
7	NH_2-MIL-125(Ti)	12	68	Xe lamp(λ > 420 nm), 300 W	[8]
8	PCN-222	1	100	Xe lamp (λ > 420nm), 100 mW/cm^2	[9]
9	PCN-822(Hf)	6	79	LED light (λ = 450 nm), 100 mW/cm^2	This

					work

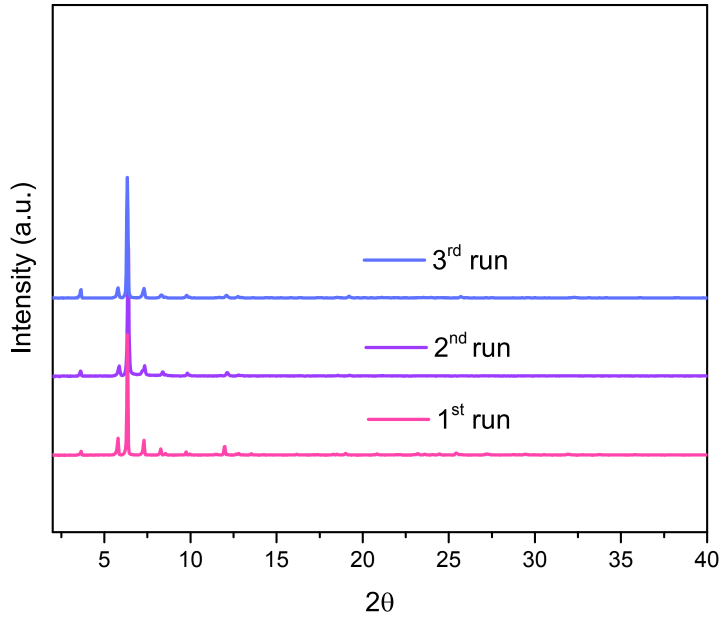

Fig. S18. PXRD patterns of recycled PCN-822 (Hf) (1st run, pink; 2nd run, violet; 3rd run, blue).

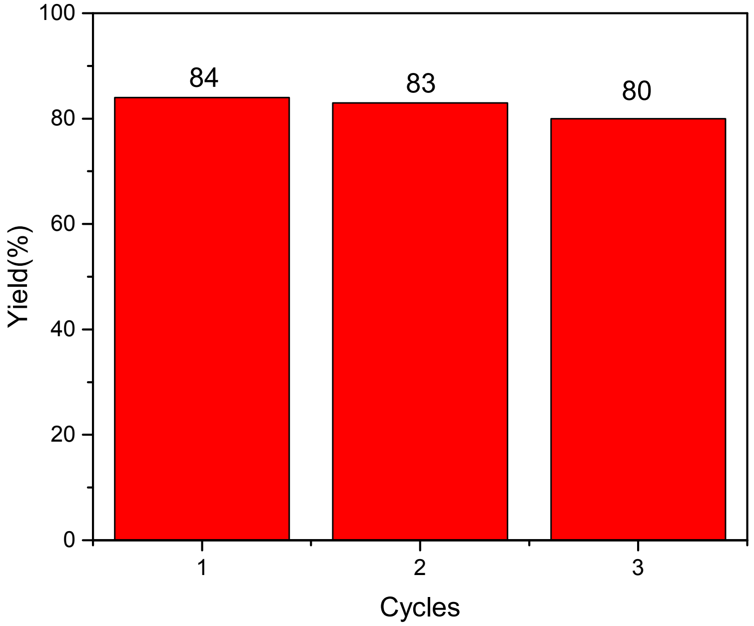

Fig. S19. Recycling performance of PCN-822 (Hf) in oxidation of dibenzylamine.

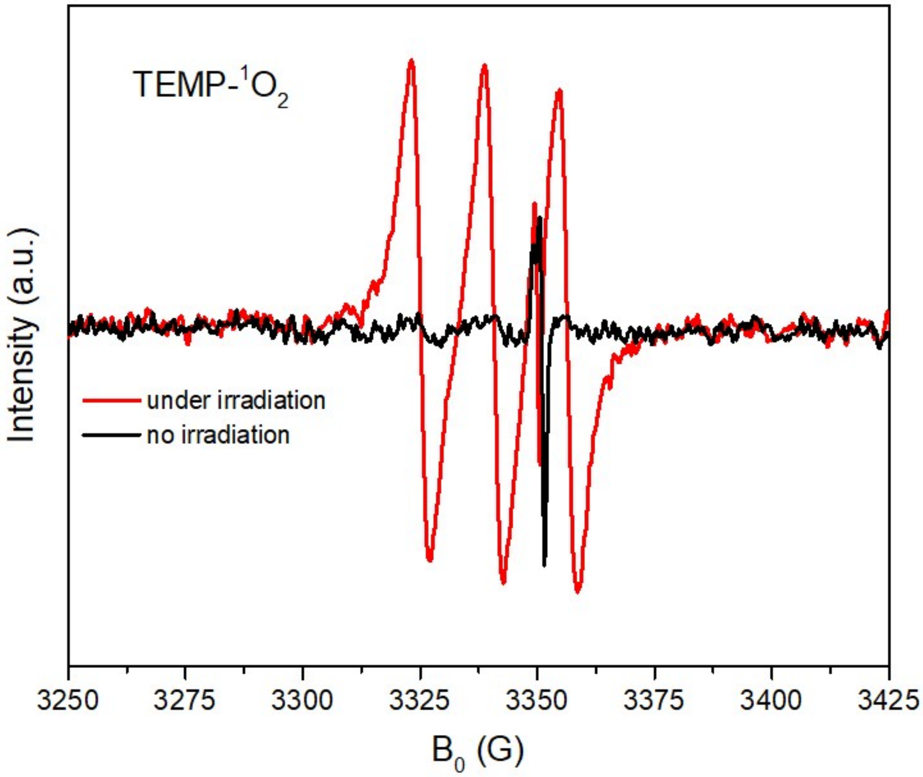

Fig. S20. EPR spectrum of TEMP-$^1O_2$.

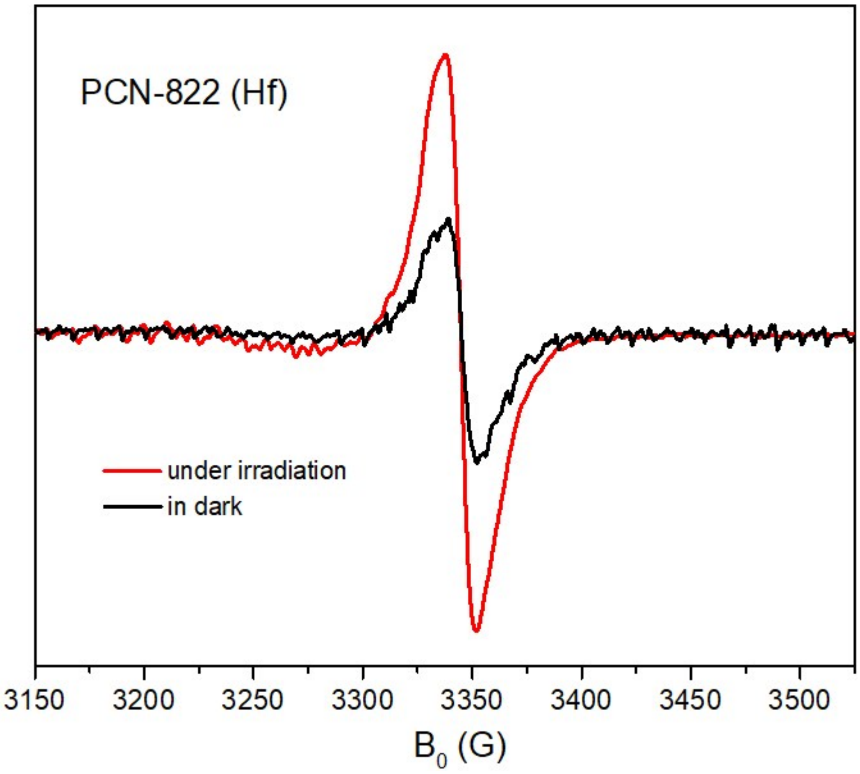

Fig. S21. EPR spectra of PCN-822(Hf) obtained in the dark and under visible light irridation.

S10. Electronic Properties

The cyclic voltammetry measurements were done with Electrochemical Analyzer from CH Instruments, inc. Platinum electrodes were used as working and counter electrodes. Ag/AgCl electrode was used as reference. The cyclic voltammograms were record in 0.1 M n-Bu_4NPF_6 solution/CH_2Cl_2 under N_2 atmosphere. All solvent used was pre-dried and degassed before use.

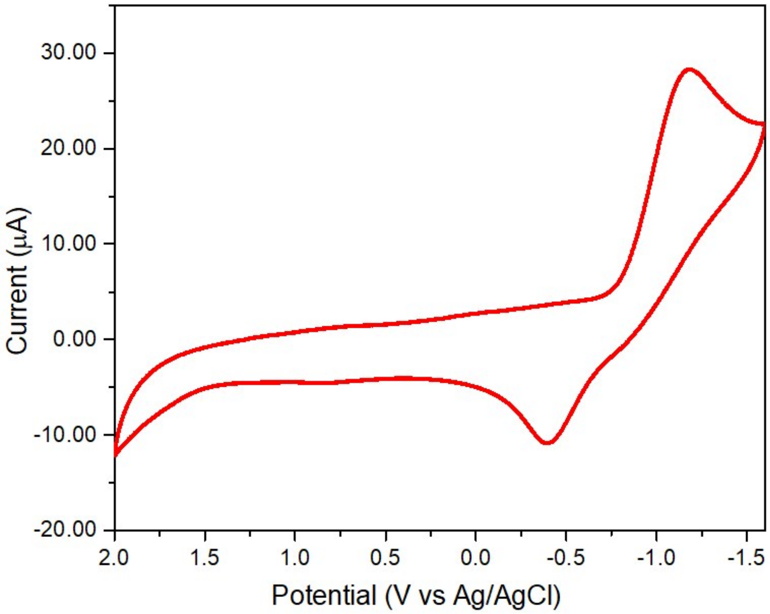

Fig. S22. Cyclic Voltammetry tests of PCN-822(Hf).

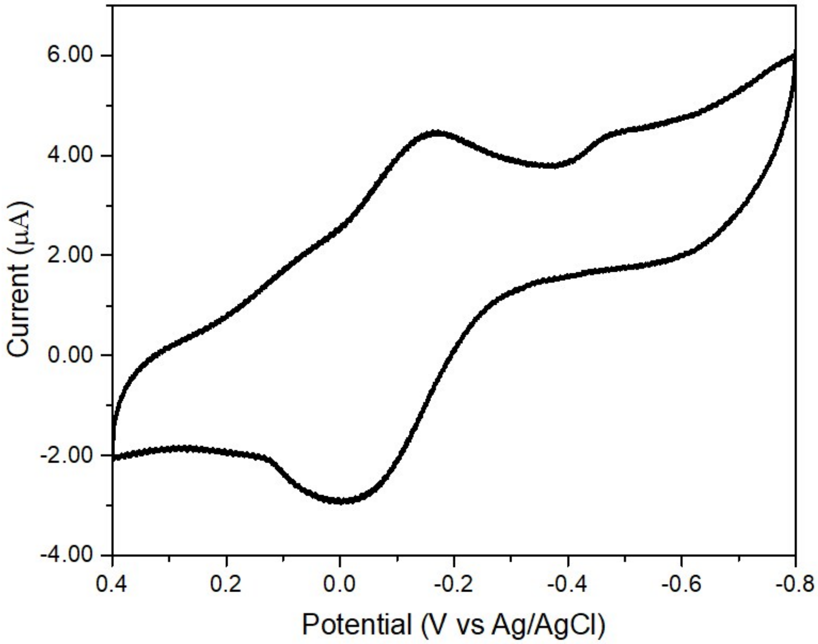

Fig. S23. Cyclic Voltammetry tests of H_4BPETB.

1. G. M. Sheldrick, *Acta Crystallogr. Sect. A: Found. Crystallogr.*, 2008, **64**, 112-122.
2. F. Raza, J. H. Park, H.-R. Lee, H.-I. Kim, S.-J. Jeon and J.-H. Kim, *ACS Catal.*, 2016, **6**, 2754-2759.
3. X. Lang, H. Ji, C. Chen, W. Ma and J. Zhao, *Angew. Chem. Int. Ed. Engl.*, 2011, **50**, 3934-3937.
4. F. Su, S. C. Mathew, L. Mohlmann, M. Antonietti, X. Wang and S. Blechert, *Angew. Chem. Int. Ed.*, 2011, **50**, 657-660.
5. G. Jiang, J. Chen, J.-S. Huang and C.-M. Che, *Org. Lett.*, 2009, **11**, 4568-4571.
6. A. Berlicka and B. Konig, *Photochem Photobiol Sci*, 2010, **9**, 1359-1366.
7. L. Huang, J. Zhao, S. Guo, C. Zhang and J. Ma, *J. Org. Chem.*, 2013, **78**, 5627-5637.
8. D. Sun, L. Ye and Z. Li, *Appl. Catal., B*, 2015, **164**, 428-432.
9. C. Xu, H. Liu, D. Li, J. H. Su and H. L. Jiang, *Chem. Sci.*, 2018, **9**, 3152-3158.